High-fat diet feeding promotes more severe and durable lung fibrotic injury in a bleomycin-induced and spirometry-confirmed mouse model of IPF

Authors
Jamal Bousamaki, Asbjørn Graver Petersen, Denise Oró, Alba Manresa Arraut, Henrik H Hansen, Michael Feigh

Gubra, Hørsholm, Denmark

Corresponding author
Michael Feigh - **mfe@gubra.dk**

BACKGROUND & AIM

Idiopathic pulmonary fibrosis (IPF) is a chronic and fatal interstitial lung disease, characterized by progressive lung fibrosis and declining pulmonary function.

The bleomycin (BLEO)-induced mouse model of pulmonary fibrosis is the most common model applied in preclinical drug discovery for IPF. However, a major limitation of the BLEO model is the spontaneous resolution of lung functional deficits and fibrosis.

Because high-fat diet intake and lipotoxicity has been implicated in IPF pathogenesis, we tested if high-fat diet feeding could promote an accelerated and more sustained fibrotic lung disease in BLEO-IPF mice.

METHODS

10-12 weeks-old male C57BL6/JRJ mice were fed normal chow (CHOW) or high-fat diet (HFD, 60% kcal of fat) for 2 weeks before receiving a single intratracheal instillation of bleomycin (1.5 mg/kg), or vehicle (sterile 0.9% saline). Mice were kept on the respective diet throughout the study. Mice were terminated 7-35 days after BLEO administration, see study outline in Figure 1. Terminal pulmonary endpoints included spirometry (flexiVent), hydroxyproline content, AI-assisted Ashcroft scoring using Gubra Histopathological Objective Scoring Technique (GHOST), quantitative histological markers of inflammation (galectin-3) and fibrosis (PSR, Col1a1, Col3, α-SMA) as well as transcriptome analysis (RNA sequencing).

www.gubra.dk

1 Study outline

Group	Animal model	Name	Number of animals
1	CHOW	CTRL	10
2	CHOW-BLEO-IPF	D7	10
3	CHOW-BLEO-IPF	D21	12
4	CHOW-BLEO-IPF	D28	12
5	CHOW-BLEO-IPF	D35	12
1	HFD	CTRL	12
2	HFD-BLEO-IPF	D7	12
3	HFD-BLEO-IPF	D21	12
4	HFD-BLEO-IPF	D28	12
5	HFD-BLEO-IPF	D35	12

Figure 1 study overview. Study outline and groups table for CHOW-BLEO-IPF and HFD-BLEO-IPF.

2 Metabolic and biochemical parameters

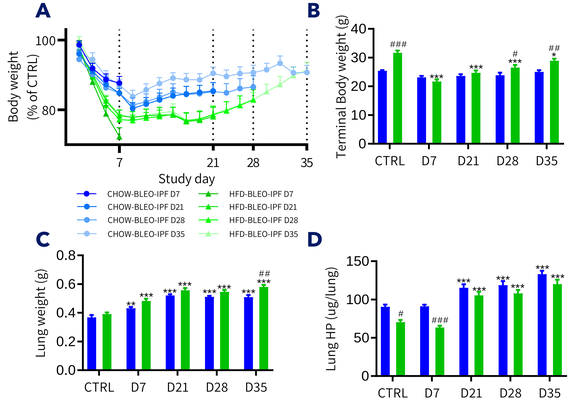

Figure 2. Metabolic and biochemical parameters. (A) Body weight change relative to baseline (% of CTRL). **(B)** Terminal body weight (g). **(C)** Terminal lung weight (g). **(D)** Terminal lung total hydroxyproline (HP) levels. Two-way ANOVA multiple comparisons analysis. *p<0.05,**p<0.01, ***p<0.001 (vs. corresponding CTRL), #p<0.05, ##p<0.01, ###p<0.001 (vs. corresponding CHOW-BLEO group).

3 Pulmonary function testing

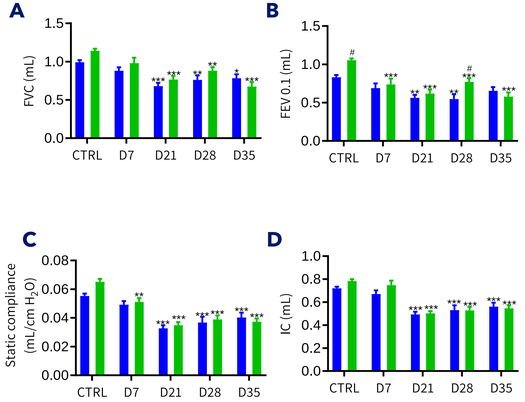

Figure 3. Pulmonary function testing. (A) Forced vital capacity (FVC). **(B)** Forced expiratory volume in 0.1 seconds (FEV0.1). **(C)** Static compliance. **(D)** Inspiratory capacity (IC). Two-way ANOVA multiple comparisons analysis. *p<0.05,**p<0.01, ***p<0.001 (vs. corresponding CTRL), #p<0.05 (vs. corresponding CHOW-BLEO group)

4 Histopathological Ashcroft scoring

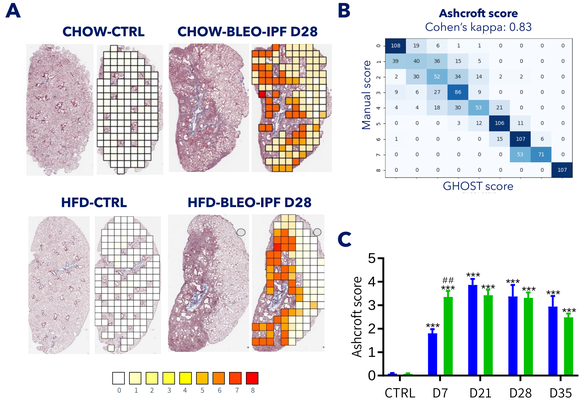

Figure 4. Automated deep learning-assisted Ashcroft scoring of lung fibrosis. Ashcroft score were determined by GHOST deep learning-based image analysis and validated against manual scoring on lung sections stained with Masson´s trichome. **(A)** GHOST-based Ashcroft scoring applied to the entire left lung in CHOW vs. CHOW-BLEO-IPF and HFD-BLEO-IPF mice terminated on study day 28. Heatmaps depict Ashcroft score (score 0-8, normal to total fibrous obliteration) in individual lung image tiles of 512x512 pixels. **(B)** Correlation of manual versus GHOST-based assessment of Ashcroft score, with the kappa value (0.83) indicating a high degree of agreement between automated and manual scoring. **(C)** GHOST-based Ashcroft scoring of mice included in the present study. Mean ± SEM. ***p<0.001 (vs. corresponding CTRL), ###p<0.001 (vs. corresponding CHOW-BLEO group). Two-way ANOVA multiple comparisons analysis**.**

5 Histological markers of inflammation and fibrosis

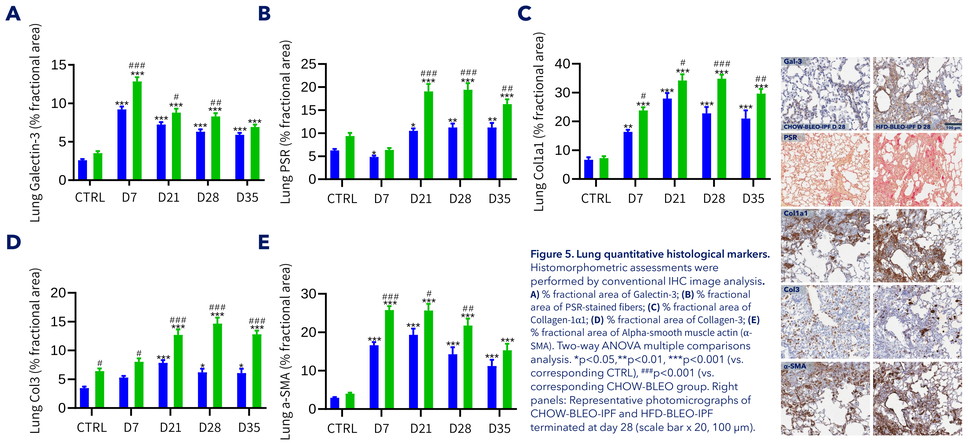

Figure 5. Lung quantitative histological markers. Histomorphometric assessments were performed by conventional IHC image analysis. **A)** % fractional area of Galectin-3; **(B)** % fractional area of PSR-stained fibers; **(C)** % fractional area of Collagen-1α1; **(D)** % fractional area of Collagen-3; **(E)** % fractional area of Alpha-smooth muscle actin (α-SMA). Two-way ANOVA multiple comparisons analysis. *p<0.05,**p<0.01, ***p<0.001 (vs. corresponding CTRL), ###p<0.001 (vs. corresponding CHOW-BLEO group. Right panels: Representative photomicrographs of CHOW-BLEO-IPF and HFD-BLEO-IPF terminated at day 28 (scale bar x 20, 100 µm).

6 Lung transcriptome signatures

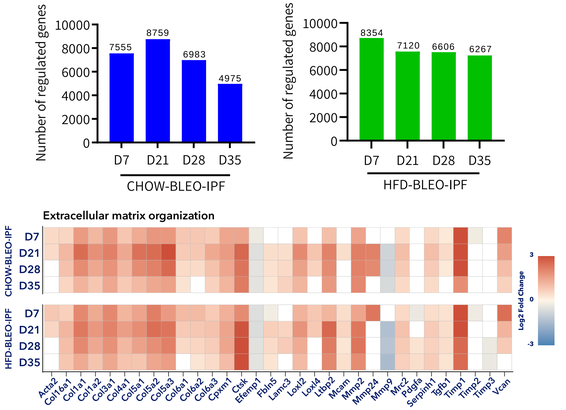

Figure 6. Lung transcriptome signatures. (A) Number of differentially expressed genes in CHOW-BLEO-IPF (left panel) and HFD-BLEO-IPF (right panel) compared to corresponding control group. **(B)** Heatmap illustrating changes in extracellular matrix-associated candidate gene expression in CHOW-BLEO-IPF and HFD-BLEO-IPF mice compared to corresponding controls. Color gradients indicate significantly upregulated (red color) or downregulated (blue color) gene expression (log2-fold change, false discovery rate < 0.05). White boxes indicate genes not significantly regulated (p>0.05). HFD-CTRL mice showed no differential gene expression compared to CHOW-CTRL mice.

Conclusion

- Both CHOW-BLEO-IPF and HFD-BLEO-IPF mice developed functional hallmarks of IPF, with a similar temporal profile in declining lung function
- Pulmonary inflammation and fibrosis was accelerated in HFD-BLEO-IPF mice compared to CHOW-BLEO-IPF mice
- Only HFD-BLEO-IPF mice maintained robust lung fibrosis from 28 days post-BLEO administration
- HFD-BLEO-IPF mice demonstrate extended duration of severe fibrotic lung injury as compared to CHOW-BLEO-IPF mice
- HFD-BLEO-IPF mice are highly relevant in preclinical target and drug discovery for IPF